Microscopic Solvation Process of Alkali Atoms in Finite Clusters: Photoelectron and Photoionization Studies of $M(NH_3)_n$ and $M(H_2O)_n$ (M = Li, Li^-, Na^-)

Ryozo Takasu,[†] Fuminori Misaizu,[‡] Kenro Hashimoto,[§] and Kiyokazu Fuke*,[†]

Institute for Molecular Science and The Graduate University for Advanced Studies, Myodaiji Okazaki 444, Japan, Faculty of Science, Tohoku University, Aramaki, Aoba-ku 980-77, Japan, and Computer Center, Tokyo Metropolitan University, Minami-Ohsawa, Hachioji-shi, Tokyo 192-03, Japan

Received: September 26, 1996; In Final Form: February 21, 1997[⊗]

Photoelectron spectra (PESs) of $Li^-(NH_3)_n$ ($n \leq 16$), $Na^-(NH_3)_n$ ($n \leq 12$), and $Na^-(H_2O)_n$ ($n \leq 7$), as well as the ionization potentials (IPs) of $Li(NH_3)_n$ ($n \leq 28$) and $Li(H_2O)_n$ ($n \leq 46$), are examined. PESs of $Li^-(NH_3)_n$ ($n \leq 10$) exhibit three bands derived from the $Li(3^2S)-Li^-(^1S)$, $Li(2^2P)-Li^-(^1S)$, and $Li(2^2S)-Li^-(^1S)$ transitions. The vertical detachment energies of the 3^2S- and 2^2P-type states decrease dramatically with increasing n. For $n \geq 11$, the transitions to the 2^2P- and 3^2S-type states almost become degenerate with the transition of the neutral ground (2^2S) state. In addition to these observations, we also find the red shift of the 2^2S-type transition with a much slower rate. The similar spectral trends are also observed for the $Na(3^2P)-Na^-(^1S)$ and $Na(3^2S)-Na^-(^1S)$ transitions of $Na^-(NH_3)_n$. On the other hand, the transitions of $Na^-(H_2O)_n$ exhibit the opposite shifts, and the $^2P-^2S$ energy separation does not change. As for $Li(H_2O)_n$, we find a monotonous decrease in IPs with $n \leq 4$ and a constant IP behavior for $n \geq 5$. The limiting value for $n \rightarrow \infty$ (3.12 eV) is comparable to the estimated photoelectric threshold of ice as in the case of $Cs(H_2O)_n$ reported previously. On the basis of these results as well as those of the *ab initio* calculations, we discuss the early stage of solvated-electron formation in finite clusters.

I. Introduction

Electrons in polar solvent have been the subject of intensive studies for the last decades.[1] Recent advances in ultrafast laser spectroscopy permit one to obtain unique information on the dynamical aspects of the solvated electron, especially on the early stage of solvated-electron formation in solution. These studies have revealed various steps in the relaxation process of the solvated electron.[2,3] In spite of these efforts, the microscopic structure and dynamics of the solvated electron in solution remain unresolved.[4] One of the most intriguing and difficult issues may be the many body interaction between a diffused electron and solvent molecules. It seems to be difficult to fully understand the solvation dynamics of the electron in polar solvent without detailed knowledge on the nature of the diffused electron. On the other hand, these issues are significantly simplified in clusters, in which the fundamental interactions in solution may be retained. The cluster study enables us a direct comparison between the experimental and theoretical results and, as a result, will provide information on the intrinsic nature of the solvated electron.

Several efforts have been made to explore the microscopic aspect of the solvated electron in clusters. Negatively charged water and ammonia clusters, $(H_2O)_n^-$ and $(NH_3)_n^-$, have been prepared via capture of low-energy electrons by solvent clusters.[5,6] The vertical detachment energies (VDEs) have been obtained for $(H_2O)_n^-$ and $(NH_3)_n^-$ with n up to approximately 70 and 1100, respectively.[7,8] The excess electron states have also been examined using quantum pass integral molecular dynamics simulations.[9,10] Moreover, the electronic spectra of $(H_2O)_n^-$ have been examined by photodestruction spectroscopy.[11] Besides these studies, the polar-solvent clusters containing neutral alkali atoms have been studied.[12,13] These clusters are the prototype of a dilute alkali metal solution, in which solvated electrons have been investigated extensively, and may serve as a good model for linking the macroscopic with microscopic properties of alkali metal−solvent systems. In these clusters, the valence electron of an alkali metal atom is expected to be transferred to a solvent cluster with sufficiently large n, and the ground state may have an ion-pair character as in the case of bulk fluids.[1] In order to probe the above transition, Hertel's and our groups have investigated the photoionization processes of the clusters consisting of alkali metal atoms such as Na[12] and Cs[13] with ammonia and water molecules. The ionization potentials (IPs) of both $Na(H_2O)_n$ and $Cs(H_2O)_n$ have been found to rapidly converge to the estimated photoelectric threshold of ice at $n = 4$ (3.2 eV),[7] while the IPs of metal−ammonia clusters decrease monotonously for n as large as 40; its limiting values again agree with the bulk photoelectric threshold of liquid ammonia at ca. 1.4 eV.[8] These features in IPs have been discussed in terms of the stabilization of an ion-pair state correlating with the solvated-electron state in bulk solution. Several theoretical groups have also made efforts to correlate the IP behaviors with the solvation state of alkali atoms.[14−20] However, since the experimental data are limited to the IP measurements, the microscopic solvation process of alkali-metal atoms in clusters has not yet been fully understood. In order to get further insight into the electronic structure of solvated alkali atoms, we have recently studied the photoelectron spectra of $Li^-(NH_3)_n$ ($n \leq 10$) produced by a laser vaporization technique coupled with a supersonic expansion method.[21] The preliminary results exhibit a rapid decrease in the energy separation between the neutral ground (^2S) and excited (^2P) states with increasing cluster size.

In the present work, we reinvestigate the photoelectron spectra of $Li^-(NH_3)_n$ ($n \leq 16$) in more detail with much better signal

[†] Institute for Molecular Science and The Graduate University for Advanced Studies.
[‡] Tohoku University.
[§] Tokyo Metropolitan University.
* Corresponding author. Present address: Department of Chemistry, Kobe University, Nada-ku, Kobe 657, Japan. E-mail: fuke@icluna.kobe-u.ac.jp.
[⊗] Abstract published in *Advance ACS Abstracts,* April 1, 1997.

S1089-5639(96)02965-9 CCC: $14.00

to noise ratio. The results clearly indicate the drastic change in the electronic structure of the 2^2P-type state as well as the higher excited state such as the 3^2S even for $n < 10$, suggesting the spontaneous ionization of the Li atom in clusters. We also examine the photoelectron spectra of $Na^-(NH_3)_n$ ($n \leq 12$) and $Na^-(H_2O)_n$ ($n \leq 7$). The spectra of the ammoniated Na^- show the similar spectral change to those for Li^-, but the hydrated Na^- exhibits no such change; for the latter clusters, both 3^2S- and 3^2P-type bands are shifted to higher VDE with a constant energy separation. In addition to these studies, we also examine the IPs of $Li(NH_3)_n$ ($n \leq 28$) and $Li(H_2O)_n$ ($n \leq 46$) to obtain further examples on the photoionization process of solvated alkali atoms. On the basis of these experimental results as well as those of the *ab initio* calculations, we will discuss the solvation state of alkali atoms in relation to the early stage of solvated-electron formation in finite clusters.

II. Experimental Section

Details of the experimental apparatus for the present photoionization and photoelectron spectroscopies have been described elsewhere.[22,23] The system for the photoionization experiments consists of a three-stage differentially evacuated chamber that includes a cluster source and a reflection-type time-of-flight (TOF) mass spectrometer. The solvent clusters containing neutral alkali atoms are produced by a supersonic expansion coupled with a laser vaporization technique. The second harmonic of a Nd:YAG laser (Quanta-Ray GCR-12) is focused onto the surface of a metal rod (5 mm diameter), which is placed in an aluminum block attached to a pulsed valve (General Valve Series 9, orifice diameter 0.8 mm). A mixture of ammonia and Ar gases is used as a carrier gas. For metal−water clusters, a reservoir is placed just behind the nozzle and is designed to be able to charge water externally. The temperatures of the nozzle and reservoir are kept at ca. 120 and 80 °C to avoid clogging of the nozzle orifice. Clusters produced are collimated with a skimmer and are introduced into the acceleration region of the TOF mass spectrometer. Clusters are photoionized with a frequency-tunable dye laser (Quanta-Ray GCR-250/PDL-3 or Lambda Physik LPX205i/FL2002). After the cluster ions are accelerated to 3 keV and are deflected and focused by ion optics, they are introduced to the reflectron TOF mass spectrometer. The mass-separated ions are detected by dual microchannel plates. The output ion signals are fed into a digital storage oscilloscope (LeCroy 9450) after being amplified by a preamplifier (NF BX-31). Photoionization mass spectra are obtained by scanning the photon energy with an interval of ca. 0.01 eV in the region of 2.23−4.56 eV (556−272 nm). The ionization thresholds are determined within ±0.03 eV by analyzing the mass spectra. The error caused by field ionization is estimated to be about 0.01 eV in the present experimental conditions.

The apparatus for the photoelectron spectroscopy consists of a three-stage differentially evacuated chamber: a negative ion beam source, a TOF mass spectrometer, and a magnetic-bottle photoelectron spectrometer. Negatively-charged solvated alkali-atom clusters are produced by the laser vaporization method. The details of the cluster source are similar to those of the $Cu^-(H_2O)_n$ clusters reported previously.[23] The second harmonic of a Nd:YAG laser (Continuum YG-661) is focused onto the metal rod (5 mm diameter), which is rotating and translating in an aluminum block. Argon gas of 2 atm mixed with water vapor or pure ammonia gas is expanded through the block from a pulsed valve (R. M. Jordan Co. PSV). Since the metal atoms (or ions) generated by the laser vaporization have a wide kinetic-energy distribution,[24] they react with solvent molecules to produce a byproduct such as the dehydrogenation products. In order to reduce the reaction, a conical nozzle, in which the laser vaporization is carried out, is attached in front of the valve. In addition, the intensity of the vaporization laser is attenuated as low as possible (less than 1 mJ/mm^2). The negative ions directly produced in the source are accelerated to ca. 800 eV in a Wiley-McLaren type TOF mass spectrometer by pulsed electric fields. The TOF mass spectrum of the nascently-produced negative ions is recorded by using dual microchannel plates placed at the end of the chamber. For the photoelectron kinetic energy measurement, negative ions with a given mass-to-charge ratio are selected with a pulsed mass gate after flying 50 cm and are decelerated to several tens of electronvolts with a pulsed potential switching method. Decelerated ions are irradiated with a detachment laser at right angles in the center of the third chamber: the third (or fourth) harmonic of a Nd:YAG laser (Quanta-Ray DCR-2A) is used for electron detachment with a typical laser fluence of ca. 5 mJ/cm^2. The magnetic-bottle type photoelectron spectrometer is used to measure the kinetic energy of the detached electron. The detached electrons are detected by dual microchannel plates after flying about 1.2 m in the electron TOF tube. The optimized magnetic fields at the detachment region and in the flight tube are about 800 and 2 G, respectively, and the resolution of the photoelectron spectra is about 120 meV for the 1.23 eV peak of the Cu^- ion with a detachment laser of 355 nm. The electron signals are accumulated as a function of flight time in a digital oscilloscope (LeCroy 7200A).

III. Results

Ionization Potentials of $Li(NH_3)_n$ and $Li(H_2O)_n$. As reported in the previous paper,[21] the $Li(NH_3)_n$ clusters are produced up to $n = 50$ the by laser vaporization technique coupled with a supersonic expansion. The mass spectrum of these cluster ions produced by the irradiation of an ArF excimer laser at 193 nm exhibits a strong magic behavior at $n = 4$. We also detect the Li_2-ammonia clusters with a magic behavior at $n = 8$. The vertical ionization potentials (IPs) of $Li(NH_3)_n$ ($5 \leq n \leq 28$) determined by the photoionization threshold measurements decrease almost linearly with $n^{-1/3}$ and give the limiting value at $n^{-1/3} = 0$ ($n \rightarrow \infty$) as 1.47 eV as shown in Figure 1. This value agrees with the limiting values for $Cs(NH_3)_n$ and $Na(NH_3)_n$ and also with the photoelectric threshold of liquid ammonia (1.45 eV).[8]

Figure 2a shows a typical mass spectrum of the clusters containing the Li atom and water molecules photoionized by 193 nm laser irradiation. $Li^+(H_2O)_n$ ions are detected for $n \leq 50$ with a strong magic behavior at $n = 4$; this magic behavior is observed even at the ionization wavelengths longer than 308 nm. The weak signals from clusters containing two and three Li atoms are also detected, but these clusters appear as the hydrogen-eliminated forms such as $Li_2^+OH(H_2O)_n$ and $Li_3^+O(H_2O)_n$, respectively. We cannot detect an aggregate such as $Li^+OH(H_2O)_n$, though the abundance of Li atoms is much higher than that of Li_2 in the present cluster source. In the literature, similar aggregates such as $Na_2OH^+(H_2O)_n$ have also been detected in sodium−water mixtures, while $NaOH^+(H_2O)_n$ have not been observed.[25] Recently, Buck and co-workers have investigated the reaction of Na_n with water clusters at the thermal collision energy using a crossed molecular beam apparatus.[26] They have found only $Na^+(H_2O)_n$ and no reaction products such as $NaOH^+(H_2O)_m$ and $Na_2OH^+(H_2O)_m$. The latter results suggest that the clusters are produced by much higher-energy collision in the present experiment: since we use the laser vaporization method to produce the Li atoms and its clusters, they may have a widespread kinetic-energy distribution.[24]

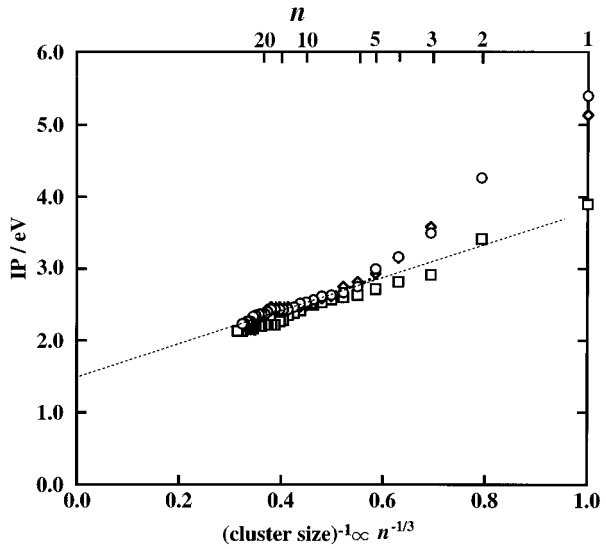

Figure 1. Ionization potentials (IPs) of $M(NH_3)_n$ (M = Li, Na, Cs) plotted as a function of $n^{-1/3}$. IPs of the Li (○) and Cs (□) systems are cited from ref 21. For comparison, IPs of Na−ammonia clusters cited from ref 12 (◇) are also plotted. The result of the least-squares fitting for $Li(NH_3)_n$ ($n \geq 5$) is also shown by the dotted line; the extrapolated value for $n \rightarrow \infty$ is 1.47 eV.

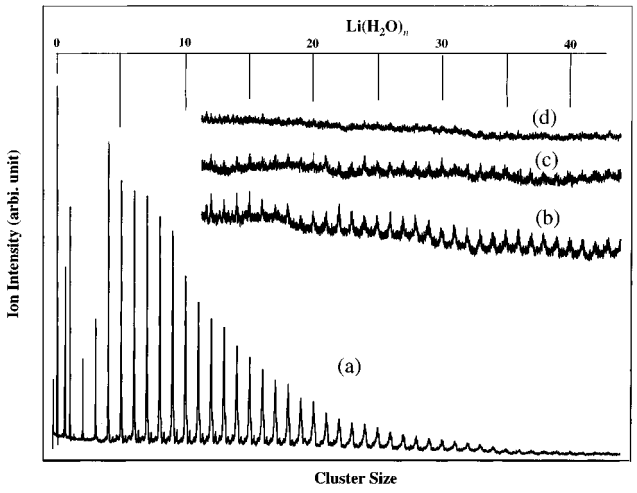

Figure 2. Typical mass spectra of $Li(H_2O)_n$ produced by photoionization at (a) 193 nm (6.42 eV), (b) 392 nm (3.16 eV), (c) 396 nm (3.13 eV), and (d) 398 nm (3.12 eV). Traces b−d are magnified at a factors of ca. 40.

In contrast to the case of the metal−ammonia clusters, the mass spectra of $Li(H_2O)_n$ show a drastic drop of the ion intensity in the ionization wavelength range from 390 to 400 nm as shown in Figure 2b−d; the ion signals for $5 \leq n \leq 46$ disappear simultaneously at 397 ± 2 nm as in the case of $Na(H_2O)_n$ and $Cs(H_2O)_n$ reported previously.[12,13] The vertical IPs for $n \geq 5$ are estimated from the ionization thresholds to be 3.12 ± 0.03 eV. We cannot determine the IPs for $n = 8$ and 9 because of the interference of coexisting background ion signals. In Figure 3, the IPs of $Li(H_2O)_n$ are plotted as a function of $n^{-1/3}$. For comparison, we also plot the results for $Na(H_2O)_n$ and $Cs(H_2O)_n$ reported previously.[12,13] The IPs of these clusters decrease almost linearly for $n \leq 4$ and become constant at 3.12 ± 0.03, 3.17, and 3.10 ± 0.03 eV for the Li−, Na−, and Cs−water clusters with $n \geq 5$, respectively. These clusters have the limiting values comparable to the estimated photoelectric threshold of ice (ca. 3.2 eV).[8]

Photoelectron Spectra of $Li^-(NH_3)_n$ and $Na^-(NH_3)_n$. Figure 4 shows the mass spectrum of the negative ions of the lithium-ammonia clusters. The spectrum consists of three series

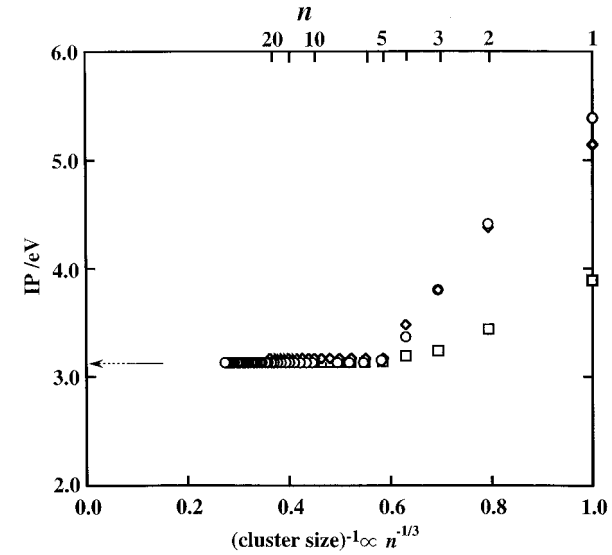

Figure 3. Ionization potentials (IPs) of $Li(H_2O)_n$ (○) plotted as a function of $n^{-1/3}$. IPs for $n \geq 5$ are 3.12 ± 0.02 eV. For comparison, IPs of $Na(H_2O)_n$ (◇) and $Cs(H_2O)_n$ (□) cited from refs 12 and 13 are also plotted.

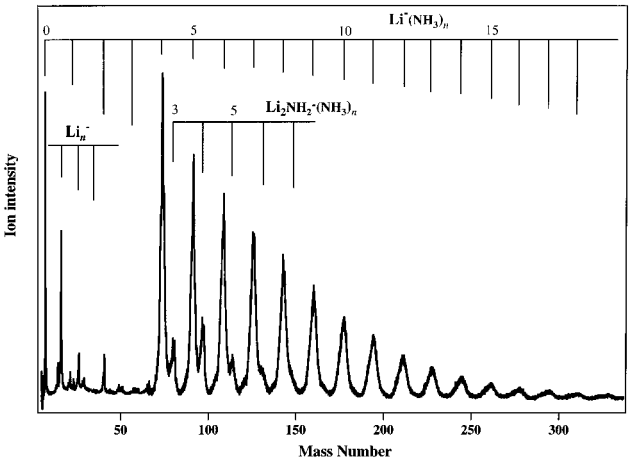

Figure 4. Typical mass spectrum of the ammonia clusters containing Li^- and Li_2^-.

of cluster ions such as Li_n^- ($n \leq 4$), $Li^-(NH_3)_n$ ($n \leq 16$), and $Li_2NH_2^-(NH_3)_n$ ($n \leq 7$). The abundance of $Li_2NH_2^-(NH_3)_n$ is estimated to be less than 20% of that for $Li^-(NH_3)_n$. The intensities of $Li^-(NH_3)_n$ decrease rapidly from $n = 0$ to 2 and exhibit a clear magic behavior at $n = 4$. Figure 5 shows the photoelectron spectra of $Li^-(NH_3)_n$ ($n \leq 16$) plotted as a function of the VDE. These spectra are recorded at the photodetachment energy of 3.50 eV. The photoelectron spectrum of Li^- consists of a strong band at 0.62 eV and a weak band at 2.47 eV, corresponding to the Li (2^2S)−Li^-(^1S) and the Li (2^2P)−Li^-(^1S) transitions, respectively. For the 1:1 complex, three peaks are observed at 0.56, 2.05, and 2.78 eV. The first two peaks correspond to the transitions to the 2^2S- and 2^2P-type states derived from those of the Li atom, respectively, while the third one is ascribed to a transition to the 3^2S-type state as discussed below. Since the abundance of $n = 2$ is very low as seen in Figure 4, it is difficult to measure the spectrum accurately; the relative intensities of the ^2S and ^2P bands contain large errors. The ^2S-type transitions of $n = 3$ and 4 shift slightly to the lower binding energy, while the ^2P-type bands of these clusters shift more rapidly to the lower energy. For the larger clusters, the ^2S-type transition stays at almost constant VDE (ca. 0.45 eV) for $4 \leq n \leq 11$ and then shifts back to the higher VDE for $11 \leq n \leq 16$. On the other

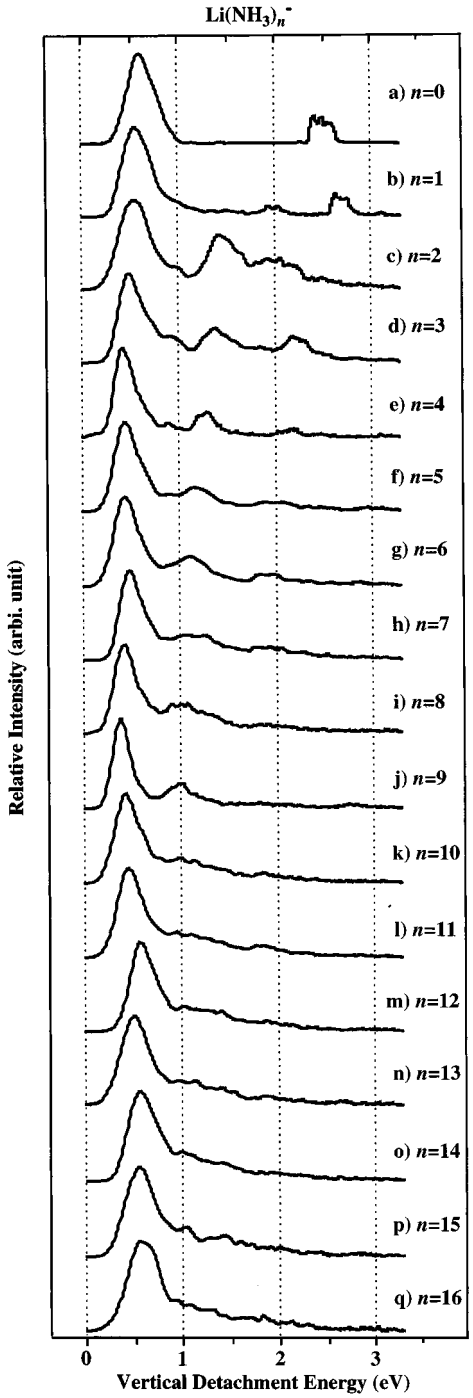

Figure 5. Photoelectron spectra of $Li^-(NH_3)_n$ ($n = 0-16$), collected using a photodetachment energy of 3.50 eV (355 nm). The spectra are normalized at the peak of the $2^2S-{}^1S$ transition.

hand, the ^2P-type transition for $n \geq 4$ shifts further to the lower energy and almost superimposes on the transition to the neutral ground state for $n \geq 10$. The 3^2S-type transition is also found to be shifted to the lower VDE and becomes much broader; the band cannot be distinguished for $n \geq 12$ and is expected to be superimposed on the 2^2P-type band. The results on the VDEs of $Li^-(NH_3)_n$ ($n \leq 16$) band positions are summarized in Figure 6.

A typical mass spectrum of negative ions of sodium−ammonia clusters is shown in Figure 7. Cluster ions $Na^-(NH_3)_n$ are mainly observed with a strong magic behavior at $n = 4$ as in the case of $Li^-(NH_3)_n$. The spectrum also contains the signals of water-mixed clusters such as $Na^-(NH_3)_{n-x}(H_2O)_x$ because of a coexistence of the trace amount of water as an impurity in

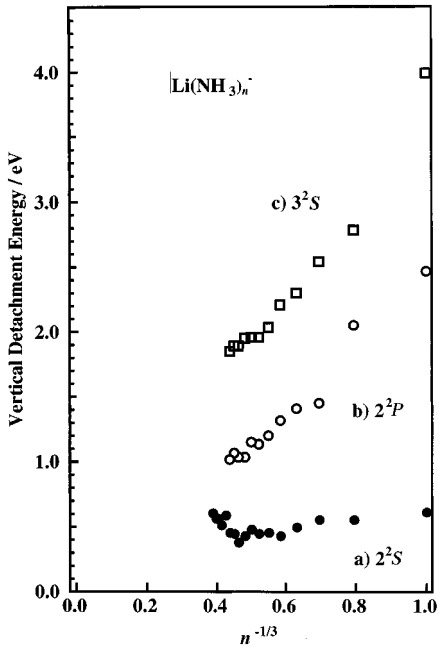

Figure 6. VDEs of the observed transitions for $Li^-(NH_3)_n$ plotted as a function of $n^{-1/3}$: (a) $2^2S-{}^1S$ (●), (b) $2^2P-{}^1S$ (○), and (c) $3^2S-{}^1S$ (□) transitions.

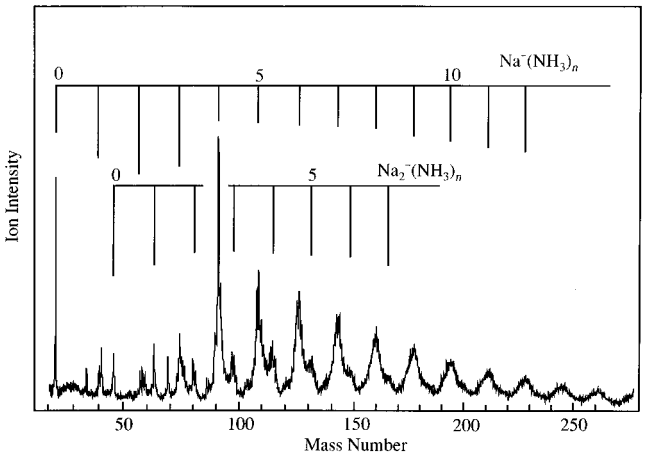

Figure 7. Typical mass spectrum of ammonia clusters containing Na^- and Na_2^-.

the sample gas line. Figures 8 and 9 show the photoelectron spectra of $Na^-(NH_3)_n$ with $n \leq 12$ obtained at the detachment energy of 3.50 eV and the observed band positions plotted as a function of n, respectively. As in the case of Li^-, the photoelectron spectrum of Na^- consists of a strong band at 0.55 eV and a weak band at 2.65 eV, corresponding to the transitions from the $Na^-(^1S)$ state to the neutral ground (3^2S) and excited states (3^2P), respectively. Although the PES of the 1:1 anion complex is rather noisy because of the low abundance of this ion in the cluster beam, the broad 3^2S-type band at ca. 0.5 eV may show the overlapping of two transitions; the main peak and shoulder are assigned to the detachment signals from two different isomers of $Na^-(NH_3)$ as discussed later. The very weak bands at near 2.4 eV can be assigned to the 3^2P-type transition, which split into two bands due to the existence of isomers. As for $n = 2$, the 3^2S-type band at ca. 0.5 eV also exhibits the broad feature probably due to the presence of isomers, while the 3^2P-type transition rapidly shifts to the lower VDE and peaks at ca. 1.7 eV. For the larger clusters, the first band is slightly shifted to the lower VDE (ca. 0.04 eV) and its bandwidth becomes smaller than those for $n = 1$ and 2. On the other hand, the bands derived from the $Na(3^2P)$ state shift

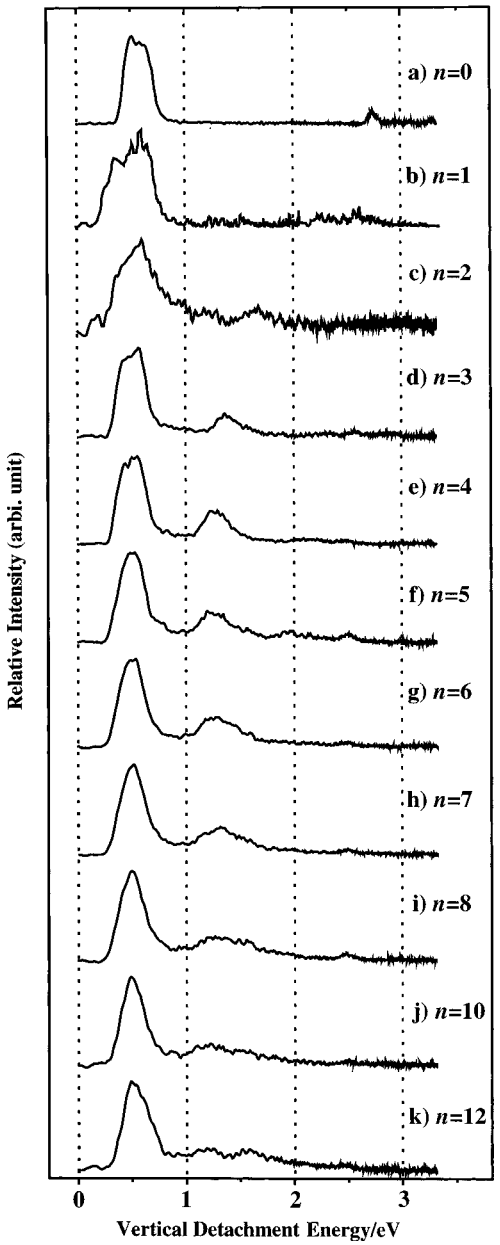

Figure 8. Photoelectron spectra of $Na^-(NH_3)_n$ ($n = 0-12$), collected using a photodetachment energy of 3.50 eV (355 nm). The spectra are normalized at the peak of $3^2S-{}^1S$ transition.

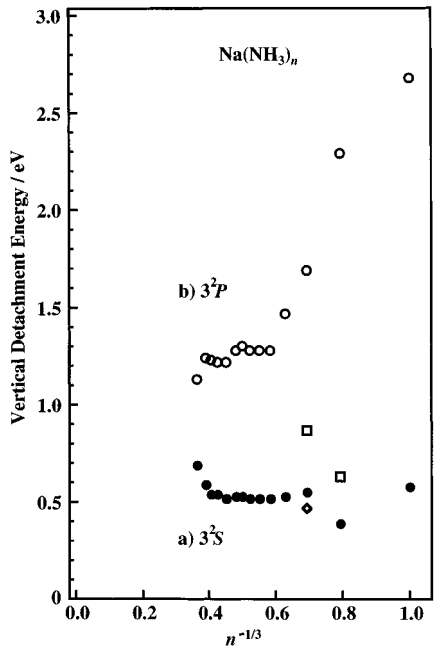

Figure 9. VDEs of the observed transitions for $Na^-(NH_3)_n$ plotted as a function of $n^{-1/3}$: (a) $3^2S-{}^1S$ (●), and (b) $3^2P-{}^1S$ (○) transitions; (□) and (◇) are the VDEs of type II and III isomers, respectively (see text).

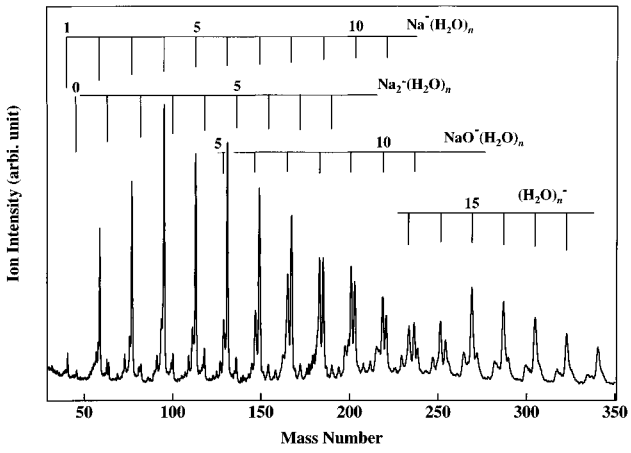

Figure 10. Typical mass spectrum of Na^-−water clusters. $NaO^-(H_2O)_n$ and $(H_2O)_n^-$ are also observed in the higher-mass region.

further to the lower VDE to about 1.2 eV. Moreover, the integrated intensity of these bands increases with increasing cluster size. As in the case of the Li^-−ammonia system, we can expect to observe the transition to the upper state derived from $Na(4^2S)$. The very weak band is observed at ca. 2.4 eV for $n \geq 5$; however, it is too weak to assign the transition to this state definitively.

Photoelectron Spectra of $Na^-(H_2O)_n$. A typical mass spectrum for the negative ions of sodium−water clusters is displayed in Figure 10. The $Na^-(H_2O)_n$ ions are observed with a magic behavior at $n = 4$. The cluster ions assignable to $NaO^-(H_2O)_n$ and $(H_2O)_n^-$ are also detected in the higher mass region. Hydrated sodium hydroxide ions such as $NaOH^-(H_2O)_n$ are found to be insignificant, which is dissimilar to the case of copper−water negative ions reported previously.[23]

Figure 11 shows the photoelectron spectra of $Na^-(H_2O)_n$ ($n = 0-7$) obtained at the detachment energy of 4.66 eV (3.50 eV for $n \leq 1$). The spectra of $Na^-(H_2O)_n$ for n up to 7 all exhibit two bands as in the case of $Na^-(NH_3)_n$, but the bands shift in the opposite direction. For the 1:1 complex, the 3^2S-type band shifts to the higher VDE by 0.21 eV with respect to the $Na(3^2S)-Na^-(^1S)$ transition at 0.55 eV. In the spectrum of $n = 2$, the former band is observed at the VDE of 0.99 eV, while the 3^2P-type band appears at ca. 3.8 eV. Both bands gradually shift further to the higher VDE with increasing n. These trends in the spectral shift are in marked contrast to those of the metal-ammonia systems. The amount of shifts for both the $3^2S-{}^1S$ and $3^2P-{}^1S$ transitions is almost the same and is as large as ca. 1.0 eV at $n = 7$ with respect to those for Na^-. Moreover, the bandwidth of the $3^2S-{}^1S$-type transition becomes much broader as n is increased through $n = 7$.

IV. Discussion

As mentioned previously, the clusters consisting of alkali-atom and polar-solvent molecules may serve as the most suitable model to explore microscopically the early stage of the solvated-electron formation in a bulk metal−solution system. In bulk fluids, alkali metals spontaneously ionize and form solvated electrons and solvated metal ions. This process may be traced

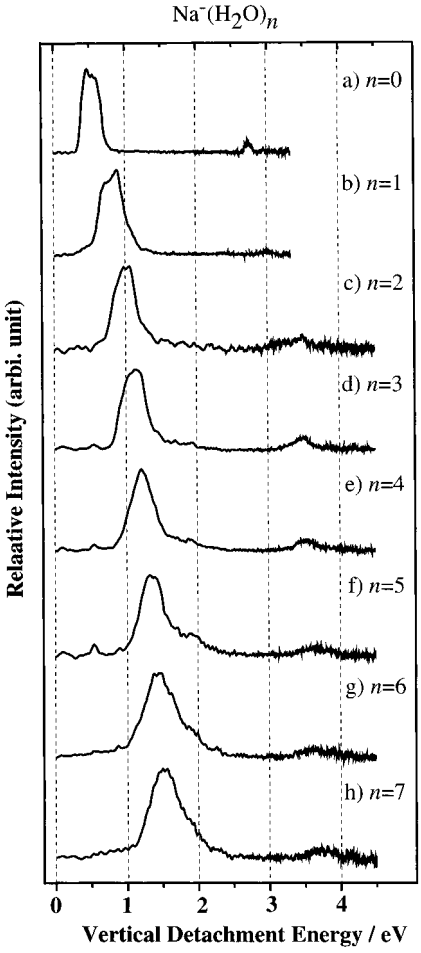

Figure 11. Photoelectron spectra of $Na^-(H_2O)_n$ ($n \leq 7$), collected using the photodetachment energies of 3.50 eV (355 nm) for $n \leq 1$ and 4.66 eV (266 nm) for $n \geq 2$. The spectra are normalized at the peak of the $3^2S-{}^1S$ transition.

in the metal−containing clusters with a stepwise manner. In order to probe the solvation state of the metal atom in clusters, Hertel's and our groups have examined the IPs of ammonia and water clusters containing Na[12] and Cs.[13] In the present work, we also study the photoelectron spectroscopy of the negative ions of these clusters. The photoelectron spectrum of the negatively-charged clusters gives information on the electronic structure of alkali atoms both in the neutral ground (^2S) and excited (^2P) states as well as the geometrical change between the anion and neutral states. In the following sections, we will discuss the solvation state of alkali atoms in detail on the basis of the results on the photoelectron and photoionization spectroscopies of these clusters and also on the *ab initio* calculations that will be reported in a separate paper.[27]

(1) Metal−Ammonia clusters. Figure 1 shows the summary of the vertical IPs of ammoniated alkali-atom clusters. Although the IPs of free atoms are different (5.392, 5.139, and 3.894 eV for Li, Na, and Cs, respectively), the size dependences of these clusters are quite similar: The IPs decrease rapidly for $n \leq 4$ and decrease further for $n \geq 4$ with a much slower rate. It is worth noticing that the IPs for $n \geq 4$ are almost the same irrespective of the kind of metal atoms, and the limiting values of IPs are in agreement with the photoelectric threshold of liquid ammonia within the experimental errors (1.40−1.47 eV). These results clearly indicate that the IPs of the clusters for $n \geq 4$ depend on the solvent molecule but not on the kind of metal atoms. In the previous paper,[13] we discussed these observations in terms of the change in the electronic character of the neutral-ground-state metal atom from the covalent-type to the one-center (Rydberg-like) ion-pair-type with increasing n. Hertel and coworkers[12] analyzed the IP results on $Na(NH_3)_n$ by solving a one-electron Schrödinger equation in a dielectrically-screened Coulomb potential. They have proposed the one-center Rydberg-like state for $n \leq 10$ and a two-center localized state for $n > 10$. Stampfli and Bennemann[16] have also calculated the IP of metal−ammonia clusters using the polarizable electropole model. Their calculations suggest the single-center structure for the intermediate size ($6 < n < 25$) and the transition to two-center structure for the larger clusters; in the latter clusters, metal ion and electron are considered to be completely separated and form two centers as in the case of bulk solution. On the other hand, one of us and Morokuma have calculated the geometrical and electronic structures as well as IPs for both $Na(NH_3)_n$ and $Na^+(NH_3)_n$ ($n \leq 6$) by using an *ab initio* method with the 6−31+G(d) basis set and the Hartree−Fock and second-order many body perturbation (MP2) methods.[20] They have found that both neutral and ion clusters with $n \geq 4$ have an interior structure where Na is surrounded by ammonia molecules. The calculations reproduce the observed IPs reasonably well and predict that the solvation energies of the cluster cations are much larger than those of the neutral clusters for $n \leq 6$, though the number of ammonia molecules in the first shell is four or five in both the neutral and ion clusters. They have also calculated the electron distribution of a singly-occupied MO (SOMO) of clusters in the neutral ground state as discussed later.

Although the above photoionization studies offer a clue to understanding the microscopic solvation process of alkali atoms in clusters, the experimental data provide information only on the energy difference between the neutral and ionic states, and thus it is difficult to obtain a deeper understanding of the solvation state of metal atoms. Moreover, as argued by Hashimoto[20] and Landman,[15] the solvation state of alkali atoms in clusters is determined by the delicate balance between the interaction of a diffused electron with the solvent molecules and the metal−solvent interaction; it seems to be difficult to describe the system using a semiempirical model potential. In order to obtain further information on the electronic structure of solvated alkali atoms, we study the photoelectron spectroscopy of ammoniated alkali-atom anions as follows.

The photoelectron spectrum of an alkali-atom anion consists of two bands due to the transitions from the ^1S anion state to the ^2S neutral ground and ^2P excited states; as shown in Figures 5 and 8, these bands are observed at the VDEs of 0.62 and 2.47 eV for Li^- and at 0.55 and 2.65 eV for Na^-, respectively. The ^2P band of these anions is much weaker than the ^2S band because it corresponds to a two-electron excitation process and is formally forbidden. For $Li^-(NH_3)$, the spectrum exhibits two bands at the VDEs of 0.56 and ca. 2.05 eV derived from the above transitions of Li^- (see Figure 5). Recently, Hashimoto and Kamimoto (HK) have calculated the geometry and electronic structure of both the negatively charged and neutral Li−ammonia clusters as well as the VDEs by the *ab initio* MO method.[28] According to the calculations at the MP2/6-311++G-(d,p) level, $Li^-(NH_3)$ has two geometrical isomers with an energy difference of 8.2 kcal/mol including zero-point energy corrections; the total binding energies of the two isomers are 11.3 and 3.1 kcal/mol, respectively. The stable isomer (type I) has the structure similar to that of the neutral complex, in which ammonia molecule is bound to Li^- by the nitrogen atom, while, in the less stable isomer (type II), NH_3 is bound to Li^- by the hydrogen atoms as in the cases of Cu^- and halide anions with water molecules.[23,29−31] The VDEs of the 2^2S state for the type I and II isomers have also been calculated as 0.44 and 0.76 eV,

respectively, at the CCSD(t)/6-311++G(d,p)//MP2/6-311++G-(d,p) level with a frozen core approximation. On the basis of these theoretical results, the peak at 0.56 eV can be assigned to the 2^2S-type transition of the more stable isomer.[31] Although theoretical results are not available, the band at ca. 2.0 eV can be tentatively assigned to the 2^2P-type transition by considering the red-shifted trend of this transition for larger clusters as seen in Figure 5. HK have also carried out similar calculations for $Na^-(NH_3)$ and found two geometrical isomers similar to the type I and II of $Li^-(NH_3)$, but with a much smaller energy difference (1.4 kcal/mol); total binding energies and VDEs of the 3^2S-type transition for the two isomers are 4.3 kcal/mol and 0.35 eV, and 2.9 kcal/mol and 0.65 eV, respectively. (The molecular geometries are optimized and total binding energies are evaluated at the MP2(all 1s frozen) level with the extended basis set including the polarization and diffuse functions. The VDEs are calculated at the CCSD//MP2 level with the same basis set.) These theoretical results suggest that the strong band and a shoulder observed at 0.6 eV and ca. 0.4 eV for $Na^-(NH_3)$ as seen in Figure 8b correspond to the 3^2S-type transitions of the unstable (II) and stable (I) isomers, respectively. The fact that the spectrum of the unstable isomer is observed with appreciable intensity for $Na^-(NH_3)$ and not for $Li^-(NH_3)$ seems to be consistent with much smaller difference in the total binding energy of two isomers for $Na^-(NH_3)$. We also observe a weak band at ca. 2.3 eV, which is tentatively assigned to the 3^2P-type transitions of the type I isomer with the same reason as that for $Li^-(NH_3)$. For $Li^-(NH_3)$, the spectrum exhibits the third band at 2.78 eV (see Figure 5b). As expected from the large shift of the ^{2}P-type transition upon complexation, an upper state such as the Li (3^2S) level, located at 3.99_3 eV above the ^{1}S anion levels, would be shifted to the present energy region. We also observe similar weak bands at ca. 1 eV above the 2^2P-type transition for $Li^-(NH_3)_n$ ($n \leq 11$) as seen in Figure 5. These arguments suggest that the 2.78 eV band of $Li^-(NH_3)$ can be assigned to the $3^2S-{}^1S$ transition corresponding to the two-electron excitation process.

As for $Na^-(NH_3)_2$, the ^{2}S-type band shows a broad feature and may indicate the presence of isomers as seen in Figure 8c. According to HK's calculations,[27] there are at least three relatively stable isomers. The more stable (I) and less stable (II) isomers have similar structures to those of the 1:1 anion complex, in which two ammonia molecules are bound to Na by the N and H atoms with C_2 symmetry, respectively; the total binding energies and VDEs of these isomers are 11.5 kcal/mol and 0.32 eV (type I), and 5.8 kcal/mol and 0.78 eV (type II), respectively. The other isomer (III) has a C_s geometry, in which one ammonia molecule is bound to Na by the N atom and the other ammonia molecule is bound to the first ammonia by N through hydrogen bond; the total binding energy and VDE are calculated to be 6.7 kcal/mol and 0.26 eV, respectively. These theoretical results indicate that the type I isomer becomes much more stable than the other isomers with increasing n and also the VDE of the isomer having N−H interaction (type II) is shifted further to the higher VDE by the ligation of ammonia molecules. The latter trend in the spectral shifts is also observed in the spectra of the Na−water systems as discussed below (see Figure 11) and due to much larger electrostatic interaction in the cluster anions than that in the neutral clusters. Therefore, the main peak at ca. 0.5 eV and the shoulder at ca. 0.4 eV can be assigned to the 3^2S-type transitions of isomers I and III, respectively, while a weak tail seen in the higher VDE region of the main peak may be tentatively ascribed to the transition of the isomer II. As mentioned previously, the ^{2}P-type transition is very weak because of its forbidden nature and also there exist isomers for small size clusters with similar binding energies. These factors as well as the low abundance of the $Na^-(NH_3)_2$ ions as demonstrated in Figure 7 make it difficult to locate the peak position of the 3^2P-type band. We tentatively assign the band at ca. 1.7 eV to this transition for the most stable type I isomer; the band shifts to the lower VDE by almost 1 eV with respect to that of Na^-. On the other hand, HK's calculations also predict three isomers for $Li^-(NH_3)_2$ having the similar structures as those of $Na^-(NH_3)_2$; total binding energies and VDEs are calculated to be 25.7 kcal/mol and 0.43 eV, 6.3 kcal/mol and 0.91 eV, and 14.2 kcal/mol and 0.31 eV for the type I−III isomers, respectively.[27] On the basis of these theoretical results, the strong band at 0.56 eV can be assigned to the transition to the neutral ground state of the type I isomer (Li^-−N interaction), while a weak shoulder at ca. 1.0 eV may correspond to the 2^2S transition of the type II isomer. As mentioned in the previous section, $Li^-(NH_3)_2$ is the least abundant ion and the relative intensity of the spectrum in the energy region above 1 eV is not accurate enough for any intensity argument. But we believe that the band at ca. 1.5 eV corresponds to the 2^2P transition of the type I isomer.

The photoelectron spectrum (PES) of $Na^-(NH_3)_3$ shown in Figure 8d exhibits two peaks at 0.51 and 1.38 eV. The spectrum exhibits an abrupt decrease in the bandwidth of the 3^2S transition from $n = 2$ to 3; the bandwidth becomes as sharp as that for Na^-. These results seem to be consistent with HK's calculations that the type I isomer of $n = 3$, in which all ammonia molecules are bound to Na by the N atom, becomes more stable than the other isomers having the Na−H bond.[28] The spectra of $Na^-(NH_3)_n$ for $n \geq 4$ also exhibit the sharp 3^2S transition and may indicate that the type I isomer is increasingly favored for the larger clusters. Thus the bands at 0.51 and 1.38 eV can be assigned to the 3^2S and 3^2P transitions of the type I isomer. As for $Li^-(NH_3)_3$, the PES shown in Figure 5d demonstrates two transitions at 0.50 and ca. 1.0 eV. Unfortunately, the theoretical results are not available for $Li^-(NH_3)_n$ ($n \geq 3$) except for the type I isomer of $n = 3$; however, the strongest band at 0.5 eV can be assigned to the 2^2S-type transition of the type I isomer ($VDE_{calc} = 0.44$ eV),[27] while the shoulder at ca. 1.0 eV may correspond to that for the type II isomer in analogy with the results on $n = 2$. The spectrum of $Li^-(NH_3)_3$ also displays the other two bands at 1.41 and 2.30 eV, which are reasonably assigned to the transitions to the 2^2P and 3^2S-type states, respectively. These bands are shifted by 1.03 and 1.69 eV with respect to those for Li^-.

The above assignments of the photoelectron spectra for both $Li(NH_3)_n$ and $Na(NH_3)_n$ with $n \leq 3$ indicate that the ^{2}S-type transition of the type I isomer having only the metal−N bond is also shifted to the lower VDE, though the amount of shift is much smaller than that for the ^{2}P-type transition; the shifts in VDE of $Li^-(NH_3)_n$ with respect to the $Li^-(^2S)$ are found to be about 0.06 and 0.12 eV for $n = 1$ and 3, while those for $Na^-(NH_3)_{1,3}$ are ca. 0.15 and 0.04 eV, respectively. These results imply that the solvation energy of the neutral clusters is equal to or larger than that in the anion state as predicted by the HK's calculations.[28] They have also calculated the electron distribution of SOMO for $Li(NH_3)_n$, and $Na(NH_3)_n$ in which the ns orbital of Li and Na is dominated, and found that the SOMO electron density for $n \leq 2$ is mainly distributed in the vicinity of the alkali atom and extends in space in the directions where NH_3 molecules do not exist. On the other hand, for $n = 3$, the SOMO density is predicted to extend in space on and between the NH_3 molecules rather than on the metal atom. These calculations suggest that the large stabilization energy of neutral clusters as large as that of the cluster anions seems to be due to

the delocalization of SOMO in addition to the metal atom−N bond formation.

As mentioned previously, the experimental and theoretical results suggest that the type I isomer having only the metal−N interaction is increasingly favored with increasing n for both the Li^-− and Na^-−ammonia systems as in the case of neutral clusters. Thus the observed photoelectron bands for $n \geq 4$ are considered to be mainly due to the transitions of the type I isomers. In other words, the photodetachment process of the clusters with $n \geq 3$ corresponds to the transition from the negative state to near the potential minimum of the neutral states. As seen in Figures 4 and 7, both $Na^-(NH_3)_n$ and $Li^-(NH_3)_n$ exhibit the magic behavior at $n = 4$. Although the clusters are generated by laser vaporization and the formation process of these clusters would be quite complex, the stability of the cluster ions may reflect on their abundance in the mass spectrum. This argument seems to suggest that $Na^-(NH_3)_4$ and $Li^-(NH_3)_4$ are more stable than their neighbors; the first solvation shell of these alkali-atom anions may be closed at $n \approx 4$. The photoelectron spectra of the Na^-− and Li^-−ammonia clusters for $n \geq 4$ exhibit the distinct features. As for $Na^-(NH_3)_n$, the 3^2P-type transition shifts further to the lower VDE for $n = 4$, and then shifts with much slower rate for $n \geq 5$ (the amount of shift of $n = 5$ is more than 1.4 eV with respect to that of Na^-). And also, its integrated intensity increases gradually with increasing n. The rapid change in the rate of shift between $n = 4$ and 5 may be ascribed to the formation of the solvation shell about Na^-. Moreover, the band width of the 3^2P-type transition increase systematically with increasing n up to 12 as seen in Figure 8, though the shift in the band position is almost the same for $n \geq 5$. These results clearly indicate that the electronic structure of the Na atom is affected further with the addition of ammonia molecules even after the first solvation shell is closed. On the other hand, the 2^2P-type transition of $Li^-(NH_3)_n$ ($4 \leq n \leq 9$) shifts to the lower VDE as large as 1.4 eV and almost becomes degenerate with the transition to the neutral ground state for $n \geq 10$ (see Figures 5 and 6). The $3^2S-{}^1S$ transition at 2.21 eV for $n = 4$ also gradually shifts further to the lower VDE up to $n = 11$ and then it smears out for $n \geq 12$. Therefore, the above results on the PES for both $Li^-(NH_3)_n$ and $Na^-(NH_3)_n$ clearly indicate the dramatic decrease in the $^2P-{}^2S$ energy separation by the ligation of ammonia molecules being coincident with the rapid decrease of IP for the neutral clusters as seen in Figure 1.

The other interesting feature of the photoelectron spectra of Li^- (Na^-)-ammonia system is that the ^{2}S-type band is also shifted slightly to the lower VDE for $5 \leq n \leq 9$ (see Figures 5 and 8). As mentioned previously, the photoelectron bands of negatively charged ions solvated in clusters generally shift to the higher VDE,[23,29−31] because of much larger solvation energy in the negative states. Thus these results are quite anomalous and indicate the larger binding energy of the neutral clusters than that of the cluster anions as in the case for $n \leq 3$ even after the first shell is closed. These results as well as the above findings that the ^{2}P-type transition is still affected for $n \geq 5$ may indicate the direct interaction of the second-shell ammonia molecules with the valence electron of the metal atom. As mentioned previously, the calculations show the extensive delocalization of the SOMO electron density of metal atom for $Li(NH_3)_3$ and $Na(NH_3)_3$. HK also found the similar delocalization of SOMO for these clusters with $4 \leq n \leq 6$.[28] If this is the case, the diffused SOMO electron may interact with even the second-shell ammonia molecules. The observations that the IPs of $M(NH_3)_n$, $n \geq 5$ (M = Li, Na, and Cs), are independent of the kind of metal atoms are also explainable by the diffused SOMO, because the electron being removed in the ionization process is considered to come from the ammonia molecules rather than the metal atom.

As shown in Figure 9, the ^{2}S-type transition of $Na^-(NH_3)_n$ ($n \geq 5$) slightly shifts back to the higher VDE. The similar shift is also observed for $Li^-(NH_3)_n$ ($n \geq 10$) as seen in Figure 6. These tendencies may be consistent with the results on the VDEs of $(NH_3)_n^-$ reported by Bowen and co-workers,[8] in which the estimated value of VDE(∞) is in agreement with the photoemission threshold of electrons from dilute metal−ammonia solution ranging from 1.42 to 1.45 eV. As mentioned previously, the ground-state $Na(NH_3)_n$ and $Li(NH_3)_n$ are the one-center (Rydberg-like) ion-pair state for smaller clusters, but it may tend to become a two-center alkali cation−surface electron state for sufficiently large clusters. If this occurs, the VDE of these clusters is expected to converge to the same limit as that for $(NH_3)_n^-$, because the interaction between the metal atom (and metal cation) and the electron in both the negatively charged and neutral states becomes negligibly small in infinite-sized clusters. The observed red shift of the ^{2}S state as well as the near degeneracy of the ^{2}S and ^{2}P states for large n may indicate that the valence electrons on the metal atom gradually move to the surrounding solvent molecules. Therefore, the present experimental results as well as the theoretical predictions suggest that the alkali atom is spontaneously ionized in rather small ammonia clusters.

(2) Metal−Water clusters. Figure 3 shows the vertical IPs of $Li(H_2O)_n$ plotted versus $n^{-1/3}$ obtained by the photoionization threshold measurements. We also plot the results for $Na(H_2O)_n$ and $Cs(H_2O)_n$ reported previously. As in the case of metal−ammonia systems, the IPs of these clusters are independent on the kind of alkali atoms for $n \geq 4$. The most surprising observation is that the IP becomes constant within the uncertainty of the photoionization threshold measurement (±0.03 eV). Moreover, the limiting value ($n \rightarrow \infty$) is comparable to the bulk photoelectric threshold of ice.[8] Until now, three theoretical groups have made efforts to interpret these anomalous IP behaviors. Barnet and Landman[15] have calculated the geometrical and electronic structures of $Na(H_2O)_n$ ($n \leq 8$) using the local spin density functional method and shown that the structure of the neutral $Na(H_2O)_n$ clusters resembles that of $Na^+(H_2O)_n$. They have also predicted that the saturation of IP for $n > 4$ is due to the formation of a molecular shell about the Na for $n \approx 4$, accompanied by exclusion of the valence electron of the alkali atom from the hydration cavity; the electron is delocalized in a surface Rydberg-like state as discussed for the metal−ammonia systems. Hashimoto and Morokuma have also investigated extensively the geometrical and electronic structures for $Na(H_2O)_n$ and $Na^+(H_2O)_n$ ($n \leq 6$) using the *ab initio* MO method.[18,19] For the neutral clusters, they have found that the most stable isomer has a surface structure, in which Na sits on the cyclic hydrogen-bonded water clusters, while, in the second stable isomer, Na is surrounded by water molecules almost tetrahedrally by the Na−O bond (interior structure). The calculated IPs for the surface isomers agree reasonably well with the observed IPs for $n \leq 6$. On the basis of these results, they have ascribed the origin of the constancy of IP to the structural feature of the surface-type isomer: In this case, the excess water molecules are bound to those in the first shell by hydrogen bond, and as a result, their effect on the local electronic structure of Na becomes much smaller for $n \geq 5$. On the other hand, recently, HK have also made *ab initio* calculations on the $Li(H_2O)_n$ clusters and found that the most stable isomers for $n \geq 4$ have the interior structure similar to those of $Li^+(H_2O)_n$ for $n \leq 6$[27] and the size dependence of their IPs agrees well with the

above experimental results. In these interior-type isomers, the SOMO electron density for $n \geq 4$ is found to be distributed not in the vicinity of Li but in the space on and between the water molecules, which suggests that the electron ejected in the photoionization process comes from water molecules being consistent with the constant IPs as shown in Figure 3. Although the metal−water clusters have been examined with various theoretical methods, it is important to carry out further study from both the experimental and theoretical standpoints to understand the size dependence of their IPs and the solvation state of alkali atom in clusters.

In order to obtain further information on the electronic structure of metal−water systems, we also carry out the photoelectron spectroscopy of $Na^-(H_2O)_n$ ($n \leq 7$). Figure 11 shows the spectra obtained at the detachment energy of 3.50 eV for $n = 1$ and 2 and at 4.66 eV for $n \geq 3$, respectively. In contrast to the case of metal-ammonia systems, both the 3^2S- and 3^2P-type transitions shift to the higher VDE by a similar amount. The spectral shifts of the former transition from that of Na^- are 0.21, 0.44, and 0.58 eV for $n = 1-3$, respectively. Similar blue shift in VDE has also been observed for $Cu^-(H_2O)_n$ in our previous work,[23] but the amounts of shift are much larger than those for the Na system (0.35, 0.73, and 1.05 eV for $n = 1-3$, respectively). Recently, Zhan and Iwata[29] have calculated the structures and VDEs of $Cu^-(H_2O)_n$ ($n \leq 2$) using the *ab initio* method. These authors have found that the Cu^- anion is symmetrically hydrated by Cu^-−H interaction; the Cu^-−H distance for $n = 1$ is 0.272 nm with the MP2 level. Their calculations (at MP4SDTQ level) reproduce the observed VDEs with reasonable accuracy. Also, the difference in the shift of VDE between Cu^-− and Na^-−water clusters has been ascribed to the radius of these ions: the ion radius has been estimated to be 0.186 and 0.265 nm for Cu^- and Na^-, respectively. As for Na^-−water clusters, HK have also calculated the structures, total binding energies, and VDEs for $n \leq 4$.[28] They have found two isomers having symmetrical Na^-−H (0.377 nm) and Na^-−O (0.233 nm) bonds for $Na^-(H_2O)$, but the former one is more stable by 1 kcal/mol. For larger clusters, HK have predicted various isomers having Na^-−H and Na^-−O interactions as well as hydrogen bonds. Among these isomers, the isomers with the Na^-−H bonds and hydrogen bonds are found to be more stable by 3−5 kcal/mol than the isomers only with Na−O bonds. These theoretical results suggest that the observed photoelectron bands are mainly due to the isomers with Na−H interactions: the origin of the blue shift in VDE is ascribed to much larger electrostatic interaction in the anion state than that in the neutral state. Therefore, these theoretical results as well as the observed trends in the PES indicate that, in contrast to the case of $Na(NH_3)_n$, the potential energy minimum of $Na(H_2O)_n$ cannot be probed by the photoelectron spectroscopy of its anions because of the large difference in the structures of the anion and neutral states. Moreover, the fact that the energy separation of the 3^2S and 3^2P states are almost the same for $n \leq 7$ as seen in Figure 11 may suggest that the electronic structure of the neutral alkali atoms is not affected appreciably by hydration when the metal−H interaction is dominant; the ns electron density is localized on the metal atom as expected from the theoretical calculations.

Although $Na^-(H_2O)_n$ is found to be not appropriate to clarify the origin of the anomalous IP behavior by the photoelectron spectroscopy, this seems not to be the case for $Li(H_2O)_n^-$. Recently, HK have also made the *ab initio* calculation for the latter clusters and found that the interior structure is the most stable in both the anion and neutral states due to the strong Li−O interactions. These results encourage us to explore the solvation state of alkali atoms in water clusters. The PES experiments of the Li−water systems are now underway in our laboratory.

V. Conclusion

The photoionization and photoelectron spectroscopies of alkali metals in polar solvent clusters have been investigated. For $Na(NH_3)_n$ and $Li(NH_3)_n$, the electronic structure of alkali atoms in ammonia clusters has been found to be extensively changed with increasing the cluster size. Especially, in the case of $Li(NH_3)_n$, the 3^2S- and 2^2P-type states of clusters are found to be dramatically stabilized and almost become degenerate with the ground state for $n \geq 10$. This trend in PES is consistent with the theoretical results that the SOMO electron density of the alkali atom is delocalized over and beyond the solvent molecules with increasing n. These results also suggest that the photoionization process of the larger clusters corresponds to the ejection of an electron delocalized over the region of solvent molecules. The observations that the Li−, Na− and Cs− ammonia clusters have the same IP value for $n \geq 5$ support the above conclusions. The present results on PES exhibit the early stage of the spontaneous ionization of the alkali-metal atom in ammonia clusters to form the one-center (Rydberg like) ion-pair state, which is the counterpart of solvated electron in finite clusters.

As for the alkali atom−water clusters, IPs are found to be independent of the kind of metal atoms and become constant for $n \geq 5$. In order to clarify the origin of these anomalous IP behaviors, we have also examined the PES of $Na^-(H_2O)_n$. Because of the large difference in the geometrical structures of the anion and neutral states, we cannot obtain information on the electronic structure of the neutral clusters. The experimental results on IPs as well as theoretical calculations seems to suggest that the alkali atom is also dissolved in small water clusters, though the solvation state of the alkali atom in water clusters is different from that in ammonia clusters due to the strong hydrogen bond in the former systems. The present study suggests that further experimental and theoretical investigations are needed to fully understand the electronic structure of the alkali atom embedded in a water cluster.

Acknowledgment. This work was partially supported by the Grant-in Aid in Priority Areas, "Chemistry of Small Manybody System" (Grants 07240102) from the Ministry of Education, Science, Sports and Culture of Japan.

References and Notes

(1) Dogonadze, R. R., Kalman, E., Kornyshev, A. A., Ulstrup, J., Eds. *The Chemical Physics of Solvation*; Elsevier: Amsterdam 1988; Part C.
(2) Gauduel, Y. In *Ultrafast Dynamics of Chemical Systems*; J. D. Simon, Ed.; Kluwer Academic Publishers: The Netherlands, 1994; pp 81−136.
(3) Alfano, J. C.; Walhout, P. K.; Kimura, Y.; Barbara, P. F. *J. Chem. Phys.* **1993**, *98*, 5996.
(4) Tuttle, T. R., Jr.; Golden, S. *J. Phys. Chem.* **1991**, *95*, 5725.
(5) Haberland, H.; Schindler, H. -G.; Worksnop, D. R. *Ber. BunsenGes. Phys. Chem.* **1984**, *88*, 270.
(6) Haberland, H.; Ludewigt, C.; Schindler, H. -G.; Worksnop, D. R. *Surf. Sci.* **1985**, *156*, 157.
(7) Coe, J. V.; Lee, G. H.; Eaton, J. G.; Sarkas, H. W.; Bowen, K. H.; Ludewigt, C.; Haberland, H.; Worsnop, D. R. *J. Chem. Phys.* **1990**, *92*, 3980.
(8) Lee, G. H.; Arnold, S. T.; Eaton, J. G.; Sarkas, H. W.; Bowen, K. H.; Ludewigt, C.; Haberland, H. *Z. Phys.* **1991**, *D20*, 9.
(9) Barnett, R. N.; Landman, U.; Cleaveland, C. L.; Jortner, J. *Chem. Phys. Lett.* **1988**, *145*, 382.
(10) Barnett, R. N.; Landman, U.; Cleaveland, C. L.; Kestner, N. R.; Jortner, J. *Chem. Phys. Lett.* **1988**, *148*, 249.
(11) Campagnola, P. J.; Lanrich, D. J.; DeLuca, M. J.; Johnson, M. A. *J. Chem. Phys.* **1991**, *94*, 5240.

(12) Hertel, I. V.; Hüglin, C.; Nitsch, C.; Schulz, C. P. *Phys. Rev. Lett.* **1991**, *67*, 1767.
(13) Misaizu, F.; Tsukamoto, K.; Sanekata, M.; Fuke, K. *Chem. Phys. Lett.* **1992**, *188*, 241.
(14) Martyna, G. J.; Klein, M. L. *J. Phys. Chem.* **1991**, *95*, 515.
(15) Barnett, R. N.; Landman, U. *Phys. Rev. Lett.* **1993**, *70*, 1775.
(16) Stampfli, P.; Bennemann, K. H. *Comput. Mater. Sci.* **1994**, *2*, 578.
(17) Hashimoto, K.; He, S.; Morokuma, K. *Chem. Phys. Lett.* **1993**, *206*, 297.
(18) Hashimoto, K.; Morokuma, K. *Chem. Phys. Lett.* **1994**, *223*, 423.
(19) Hashimoto, K.; Morokuma, K. *J. Am. Chem. Soc.* **1994**, *116* , 11436.
(20) Hashimoto, K.; Morokuma, K. *J. Am. Chem. Soc.* **1995**, *117*, 4151.
(21) Takasu, R.; Hashimoto, K.; Fuke, K. *Chem. Phys. Lett.* **1996**, *258*, 94.
(22) Misaizu, F.; Sanekata, M.; Tsukamoto, K.; Fuke, K.; Iwata, S. *J. Phys. Chem.* **1992**, *96*, 8259.
(23) Misaizu, F.; Tsukamoto, K.; Sanekata, M.; Fuke, K. *Laser Chem.* **1995**, *15*, 195.
(24) Sanekata, M.; Misaizu, F.; Fuke, K.; Iwata, S.; Hashimoto, K. *J. Am. Chem. Soc.* **1995**, *117*, 747.
(25) Schultz, C. P.; Haugstätter, R.; Tittes, H.-L.; Hertel, I. V. *Z. Phys.* **1988**, *D10*, 279.
(26) Bewig, L.; Buck, U.; Rakowsky, S.; Reymann, M.; Steinbach, C. In *Abstracts of the 8th International Symposium on Small Particles and Inorganic Clusters*; Lindelof, P. E., Ed.; University of Copenhagen: Denmark, 1996.
(27) Hashimoto, K.; Kamimoto, T. To be submitted.
(28) (a) Hashimoto, K.; Kamimoto, T. *Structure and Dynamics of Clusters, Proceedings of the Yamada Conference XLIII* 1995; Kondow, T., Kaya, K., Terasaki, A., Eds.; Universal Academy Press: Tokyo, 1996; pp 563−572, pp 573−580.
(29) Zhan, C.-G.; Iwata, S. *Chem. Phys. Lett.* **1995**, *232*, 72.
(30) Markovich, G.; Giniger, R.; Levin, M.; Cheshnovsky, O. *J. Chem. Phys.* **1991**, *95*, 9416.
(31) Arnold, D. W.; Bradforth, E. H.; Kim, E. H.; Neumark, D. M. *J. Chem. Phys.* **1995**, *102*, 3510.
(32) A weak tail observed in the higher VDE region of the 0.56 eV band (see Figure 5b) may correspond to the 2^2S transition of the type II isomer; however, we cannot conclude definitively with the present PES resolution.